Int j simul model 24 (2025) 4, 647-658
Original scientific paper

PARAMETER OPTIMIZATION OF ROTARY BLADE FOR SOIL BREAKAGE USING DISCRETE ELEMENT METHOD

Fu, C. G.[*]; Wang, Q. F.[**]; He, W. W.[***,#]; Lv, W. Q.[****] & Wei, S. X.[*]
[*] School of Mechanical Engineering, Guizhou University of Engineering Science, Bijie 551700, China
[**] School of Biological Engineering, Xinxiang University, Xinxiang 453000, China
[***] School of Mechanical Engineering, Hebei University of Technology, Tianjin 300380, China
[****] College of Engineering, China Agricultural University, Beijing 100083, China
E-Mail: wei989926@163.com ([#] Corresponding author)

Abstract

This study aims to improve rotary tillage quality in Chinese loess areas by optimizing parameters of the rotary blade for enhanced soil particle breakage. A 3D model of the standard IT245 rotary blade and blade roller was established in SolidWorks, and simulation experiments under multiple parameters were conducted via the Discrete Element Method for the blade roller-soil interaction system, with the soil particle breakage effect as the evaluation index. The effects of the two parameters on soil breakage and optimization effectiveness were analysed. Results reveal that, the bending angle has a more significant impact on the soil breakage effect than blade tip thickness, and the most optimal parameters are 54° bending angle and 3.0 mm blade tip thickness. Compared with the normal parameters (60°, 3.0 mm), the average number of particles increases by 5.14 %, small unit mass particles (Sections 1 and 2) increase significantly, the total mass ratio of large particles (Sections 3-7) is the lowest, and the soil breakage effect is effectively improved. This obtained conclusions provide a reliable simulation basis for rotary blade parameter design in loess areas.

(Received in September 2025, accepted in October 2025. This paper was with the authors 1 week for 1 revision.)

Key Words: EDEM, Soil Breakage, Rotary Blade, Bending Angle, Blade Tip Thickness

1. INTRODUCTION

With the global population growth and the intensification of cultivated land resource constraints, improving agricultural productivity has become a key challenge to ensure food security [1, 2]. The high-intensity agricultural production mode leads to soil structure compaction, organic carbon loss, and functions degradation. *The Statistics of the World Soil Resources Status Report* reveals the serious average annual erosion rate of global cultivated land. The global cumulative yield loss may reach 10.25 % from 2015 to 2050, which is equivalent to the function loss of 150 million hectares of cultivated land [3]. In "The 14th Five-Year Plan" of China, the implementation of the cultivated land quality improvement project has been proposed to strengthen the efficient use of soil resources [4]. As an important index for evaluating soil structure, the soil fragmentation rate directly affects soil aeration, root growth, and crop nutrient absorption [5-7]. Optimizing the soil breakage quality and improving its mechanical-physical properties are of great value for increasing crop stress resistance, enhancing yield stability, and promoting agricultural low-carbon development. Therefore, deeply probing into the soil breakage rate from the perspectives of mechanical engineering and soil dynamics and developing suitable farming machines and techniques will be of remarkable theoretical and engineering value for improving the quality of cultivated land and ensuring food security.

Soil degradation manifests primarily at the mechanical level as soil structure instability, loss of organic matter, and reduced shear strength and erosion resistance [8]. To address such problems, researchers have been dedicated to the soil improvement of cultivated land by optimizing tillage techniques [9, 10]. The operating quality of rotary tillage, the main tillage mode, directly affects the soil structure improvement and root growth environment [11]. As a key index for evaluating the rotary tillage effect, the soil breakage rate decides the aggregate distribution in the plowing layer and the soil structural stability. The geometric parameters (e.g., bending angle and blade tip thickness) of rotary tillage tools regulate soil cutting, breaking, and motion and further affect the configuration of soil aggregates [12]. Therefore, systematic research on the action mechanism of tools' geometrical parameters on the soil breakage rate is of great engineering and theoretical value for optimizing tillage tools, improving soil quality, and delaying soil degradation.

In this study, the breakage rate of soil is explored by simulating the soil-rotary tiller interaction using the discrete element method. Soil is deeply cut using the rotary tiller in the motion process, and the breakage rate is elevated by introducing different blade bending angles and blade tip thicknesses to solve the problem of the low breakage rate during soil deep tillage, contribute to mitigating soil degradation, and render favourable design parameters for the rotary tiller in agricultural deep tillage.

2. STATE OF THE ART

At present, the main measures to improve soil quality are no-tillage, cover crops, straw incorporation, and deep tillage. Given the complexity of the soil structure, appropriate improvement measures should be chosen according to the structural characteristics of soil [13]. Deep tillage mainly refers to soil cutting, breaking, and mixing through the high speed rotating blades of a rotary tiller, which can markedly improve soil quality and enhance soil productivity potential [14]. Therefore, broad application prospects are expected in soil improvement based on soil deep tillage using rotary tillers.

To select the rotary blades adaptable to specific tillage conditions and optimize their performance, a large number of experiments are needed to quantify the coupling effect between key geometric parameters accurately, such as blade bending angle, blade tip thickness, and soil fragmentation rate. However, this process involves complex multifactor dynamic coupling, and the traditional experimental methods are expensive and lengthy. Therefore, the Enhanced Discrete Element Method, EDEM-based numerical simulation has developed into a highly potential research path and attracted numerous scientific researchers [15, 16]. Studies have shown that the geometrical configuration and motion parameters of tillage tools substantially affect the composition and structural stability of soil aggregates. For instance, Nalawade et al. [17] systematically analysed the influence of the sweep angle of the rotary tiller and its interaction with operating parameters such as forward speed and rotation speed on tillage performance through discrete element simulation and soil bin tests and provided guidance for understanding the tool-soil interaction to elevate the breakage rate. In a sandy soil environment, Xiao et al. [18] optimized the macroscopic structural parameters of the rotary blade, including the tangential bending radius, bending angle, and edge thickness, through numerical simulation, demonstrating a reduction in cutting resistance and a 2.4 % decrease in power consumption. However, the effect of these parameters on soil fragmentation was not examined. Similarly, Zhao et al. [19] employed the discrete element method (DEM) to investigate the influence of the blade's side-curve angle, finding that a larger angle reduced both torque demand and soil disturbance. Nevertheless, the impact of blade thickness was not considered in their study. In terms of model applicability, Sun et al. [20] applied the Hertz–Mindlin contact model to simulate the interaction of bionic deep plows and common deep ploughs with soil comparatively, accurately measured the working force and energy consumption, analysed the characteristics of soil disturbance, and successfully verified the reliability and applicability of the model in multiparticle mixing and stirring simulation. Generally, the operating parameters of rotary blades have been extensively studied, but more attention is paid to the stress, cutting length, and cutting width in the cutting process; a systematic analysis regarding the influence of the rotary blade's bending angle and blade tip thickness on the soil breakage rate is lacking. Further systematic research is urgently needed in this field to establish an accurate correlation between tools' geometric parameters and soil breakage quality and to provide a solid theoretical basis and engineering guidance for optimizing tillage tools, improving soil quality, and curbing soil degradation.

At present, global available arable land is influenced by geographical location, topography, and other factors, which form soil mechanical profiles and physical configurations with considerable regional heterogeneity. The heterogeneity directly determines the requirements for the adaptability of the tillage mode and machine tool system. In loess areas, such as the North China Plain in China, the long-term adoption of shallow rotary tillage easily induces the plow pan formation and interface hardening and substantially hinders water infiltration and root mechanical penetration; thus, it has become the key mechanical limiting layer that restricts the improvement of crop productivity [21-23]. Precisely regulating soil fragmentation rates by optimizing rotary tillage parameters according to the mechanical properties of soils in different regions represents a critical engineering technique for enhancing soil quality and reversing degradation trends in the global effort to combat soil degradation.

The above research results mainly examined the cutting length, cutting width, and mechanical properties of rotary blades. On the one hand, rotary blades have been widely applied in deep tillage, but the soil breakage rate achieved by rotary blades has not been fully investigated. On the other hand, the soil characteristics in different areas remain to be explored further due to the complex topographical conditions on a global scale. Thus, this study focuses on the standard rotary tiller blade IT245. Using the soil characteristics of the North China Plain as an example, this study comprehensively employs SolidWorks 3D modelling and EDEM discrete element simulation technology to construct a numerical simulation platform based on the Hertz-Mindlin with JKR contact model and the Tavares UFRJ fragmentation model. By simulating various parameter combinations for conventional tillage operations through system modelling, this study aims to elucidate precisely the mechanism by which bending angle and blade tip thickness influence soil fragmentation rates. Based on these findings, this study optimizes the parameters to provide critical theoretical support and practical guidance for designing efficient, low-consumption rotary tillage tools.

The remainder of this study is organized as follows: In Section III, the structure and working principle of the rotary blade are introduced. In Section IV, the tool-soil interactions under different working conditions are investigated. In Section V, the overall research work is reviewed, and this study is summarized to provide valuable reference for optimizing the soil breakage rate from different bending angles of the rotary blade.

3. METHODOLOGY

In this section we describe our proposed service discovery framework and its architecture. Most existing service search and discovery technologies are based on keyword search. Although keyword-based service discovery could provide users with related services, the probability of failing to find services that satisfy most or the main components of the customer's requirements is high. In this research, we propose an intelligent service discovery method that provides users with service search results based on a comparison of users' requirements with advertised services, as well as the characteristics and structure of service semantic features analogous to those of service ontology.

3.1 Model selection and modelling of the rotary blade

The standard IT245 rotary blade, which is made of 65Mn, with a bending angle of 60° and a blade tip thickness of 3.0 mm, was taken as the study object. The standard IT245 rotary blade was modelled in SolidWorks, as shown in Fig. 1.

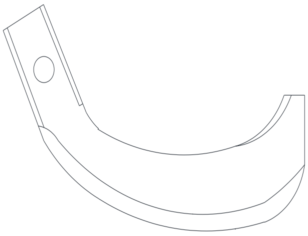

Figure 1: Overall view of the blade.

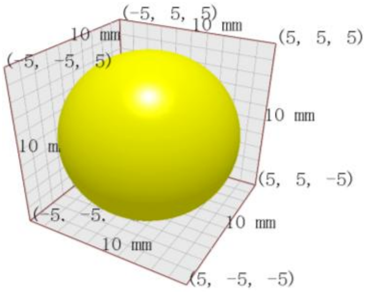

Figure 2: Soil particle model diagram.

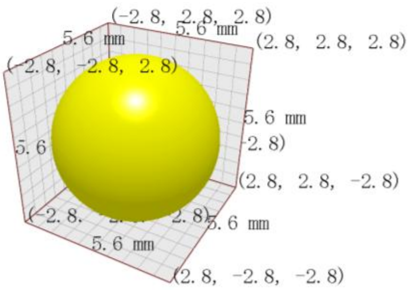

Figure 3: Passivator model rotary diagram.

3.2 Model setting

Soil model setting: The morphology of soil particles was simulated using a smooth solid sphere model. The Single Sphere particle model was chosen from the particle model library of EDEM2020 software, and the radius of the soil particles was set to 15 mm. The radius of the soil particle was set to 5 mm, as shown in Fig. 2 and the simulation model and random distribution parameters are illustrated in Fig. 3.

Particle materials and settings of contact property parameters: The material property parameters of soil and the rotary blades and the contact property parameters between particles and those between particles and the rotary blades are listed in Table I.

Table I: Particle material and contact properties of interactive materials [24].

Material	**Poisson's ratio**	**Density** (kg/m^3)	**Shear modulus** (Pa)	**Interactive materials**	**Restitution coefficient**	**Static friction coefficient**	**Rolling friction coefficient**
Soil	0.4	1346	1×10^6	Soil–soil	0.2	0.4	0.3
65Mn	0.35	7830	7.27×10^{10}	Soil–65Mn	0.3	0.5	0.05

3.3 Geometrical model for simulation

The rotary blades and blade roller were combined into a whole for the simulation. A 450×600×650 mm soil trough was established to wrap the soil particle model (shaded area in Fig. 4) according to the working width of the blade roller and the tillage depth of 250 mm, and a 400×600 mm dummy plane was built on the top of the soil trough as the particle factory to produce particles. The motion velocity of the rotary blade roller was subject to the motion velocity of the standard rotary tiller, the linear motion velocity was set to 3 km/h, the rotational speed was set to 250 r/min. The rotary blade roller and the housing were set to move forward along the negative direction of the Y-axis. According to the soil mass volume and the volume of soil to be filled, the total mass of particles input by the particle factory was solved as 2300 kg, and the input velocity was 2300 kg/s; thus, the particle input was completed within 1 s. The resulting model is shown in Fig. 4.

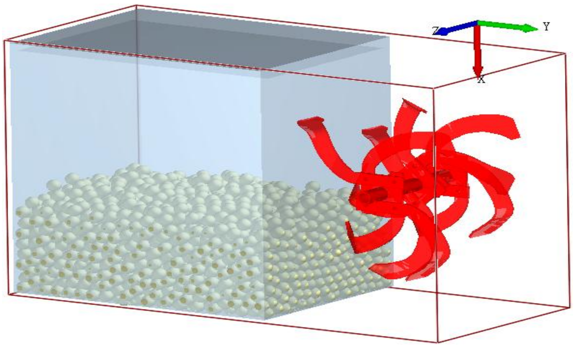

Figure 4: Soil breakage model of the rotary blade.

3.4 Rotary tillage model setting

In the simulation experiment, the Hertz-Mindlin with JKR contact model in the contact model library of EDEM software was selected, and the bonding energy of soil particles was set to 8 J/m^2 [25]. The Tavares UFRJ was selected as the breakage model, and its parameters are shown in Table II. To ensure the reliability of the simulation results and to simulate soil breakage by the rotary blade in a realistic environment, the gravity environment of the particle model was set to -9.81 m/s^2 in EDEM [26]. Based on the rotary blades' travel velocity of 0.83 m/s and the spindle speed of 4.2 r/s, the simulation time was set to 3.3 s, the data saving interval was set to 0.01 s, the grid size was set to 3 R/min, and the time step was set to 19 %.

Table II: Tavares UFRJ parameter settings.

Tavares breakage model parameters	Tavares breakage model parameter settings	Tavares breakage model parameters	Tavares breakage model parameter settings
Damage Constant	5	Alpha Percentage	67
Global Damping Time	0 s	B	0.029
Global Damping Str.	0	D Minimum	3.0 mm
E Infinity	17 J/kg	E Minimum	0.0001 J
D_0	8.07 mm	C_T	0
Phi	1.22	Truncation Ratio	100
Std Deviation	0.799		

3.5 Simulation of soil breakage by the rotary blade

Based on the standard IT245 rotary blade (bending angle: 60° and blade tip thickness: 3.0 mm), the rotary blades with bending angles of 48°, 50°, 52°, 54°, 56°, 58°, 60°, 62°, 64°, and 66° were designed for the EDEM simulation experiments with reference to the *Rotary Tiller* (GB 5668-2017) [27]. Considering the actual operating conditions, the tillage depth was set to 250 mm in the simulation experiment, the dry tillage velocity to 3 km/h, and the spindle speed of the rotary blades to 250 rpm, and each set of simulations was repeated 10 times. The particle number in each experiment was summed to obtain the total particle number, and the average value was calculated after excluding the maximum and minimum values. The mass of particles with Specifications 1–7 (the masses of 5.58×10^{-5}, 3.35×10^{-5}, 6.70×10^{-5}, 1.3×10^{-5}, 2.3×10^{-5}, 3.69×10^{-5}, and 6.37×10^{-5} kg) in each experiment was multiplied by the corresponding particle number to obtain the total mass of particles of each specification, and the maximum value and minimum value of the data obtained in 10 experiments were excluded to calculate the average value. The EDEM simulation experiments were performed using the blades with the optimal bending angle and with designed blade tip thicknesses of 2.0, 2.5, 3.0, 3.5, and 4.0 mm, and other conditions were unchanged.

To analyse the breakage degree of soil particles under rotary blades operation, particle “soil” was set to “mass” in postprocessing, and the vector showed that differently coloured spheres represent broken particles with different masses. A further analysis was performed using the data after experiment at 2.5 s of the bending angle of 50° and blade tip thickness of 3.0 mm, 62° and 3.0 mm, and 54° and 4.0 mm. The optimized blade parameters were input into SolidWorks for modelling.

4. RESULTS AND DISCUSSION

Following the work plan in Sections 3.2–3.5, loess from the North China Plain was used as the test material to investigate the relationship between blade parameters and soil breakage.

4.1 Data analysis of rotary blades with different bending angles and blade tip thickness of 3.0 mm

Fig. 5 shows that at the bending angle of 48°–66°, the overall total particle number first increased and then decreased as the bending angle of the rotary blade increased. In experiments 1–7, the total particle number reached its maximum at a bending angle of 54°, whereas in the 8th experiment, the maximum occurred at 52°. The data of 8 experiments were averaged, and the total particle number was maximized at the bending angle of 54°. As seen in the broken line graph, the increasing bending angle had a greater effect on the total particle number than the declining bending angle, with 54° (the bending angle corresponding to the maximum total particle number), as the baseline.

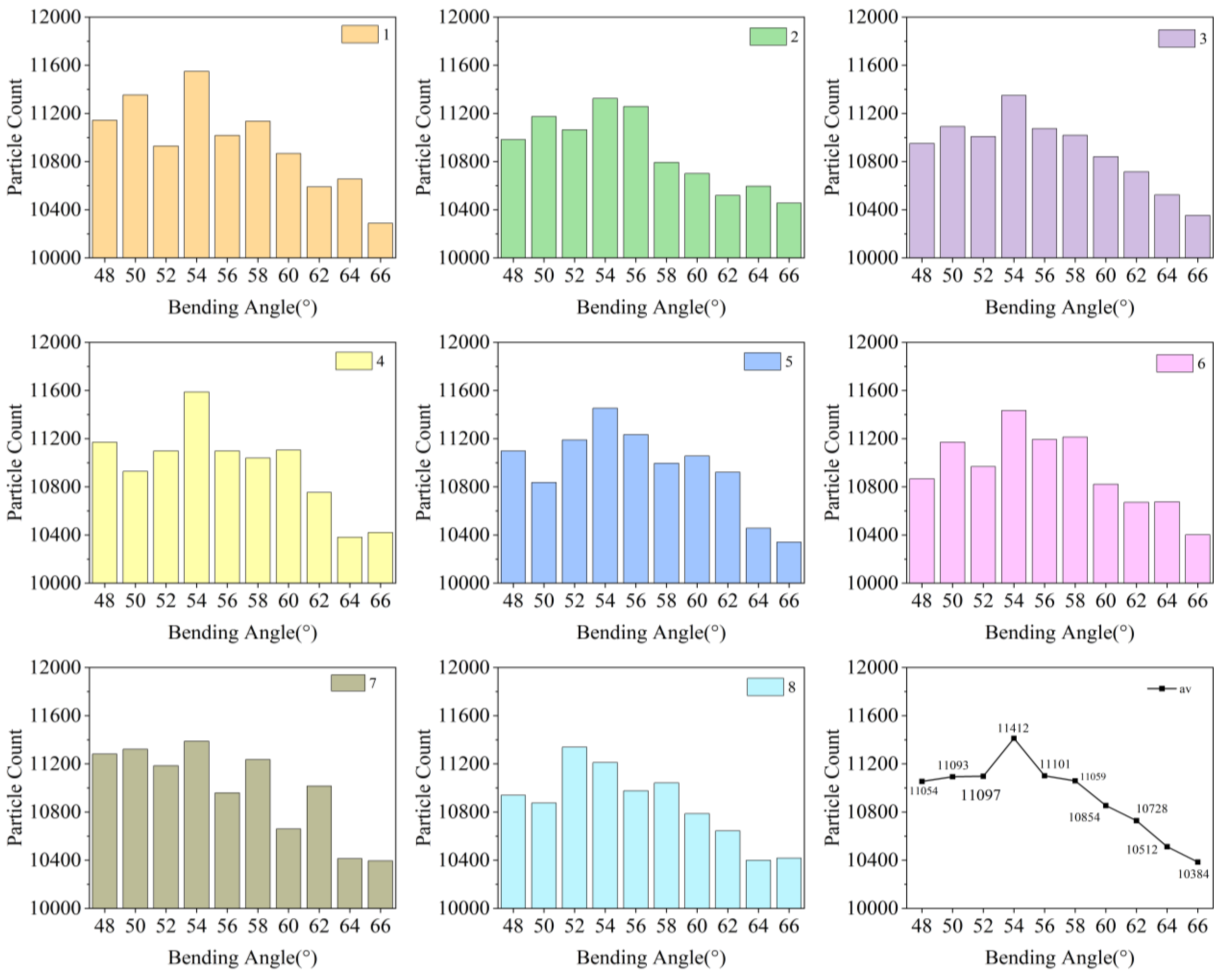

Figure 5: Influence of bending angle on total particle mass.

Fig. 6 shows that the particle mass of Specifications 1–7 presented a gradual increasing trend at the bending angle of 48°–66°. As the bending angle increased within the range of 48°–66°, the particle mass of the Specifications 1 and 2 first increased, then decreased, and peaked at 54°; the particle mass from Specifications 3–7 first decreased and then increased, where the particle mass of Specifications 3, 4, 5, and 7 reached its minimum value at 54°, and that of Specification 6 touched the bottom at 56°. Fig. 7 indicates that the particle number of Specification 1 was much greater than that of other specifications at the bending angle of 48°–66°, followed by that of Specification 7. A combined analysis of Figs. 6 and 7 reveals that the particle number of Specification 1 was always the greatest among all particle specifications across the 48°–66° bending angle range, and it peaked at the bending angle of 54°; the particle mass of Specifications 3, 4, 5, and 7 reached their bottom at the bending angle of 54°, that is, high-mass particles accounted for the lowest proportion in the total mass of particles of all specifications. In summary, Specifications 1 and 2 had the lowest individual particle mass. The combination of low particle mass and high particle number indicated a good breakage effect and suggested that the breakage of small-mass particles is most favourable at a bending angle of 54°. The total particle number was the highest at the bending angle of 54°, and high-mass particles accounted for the lowest mass ratio; thus, the bending angle of 54° was selected for the follow-up experiments.

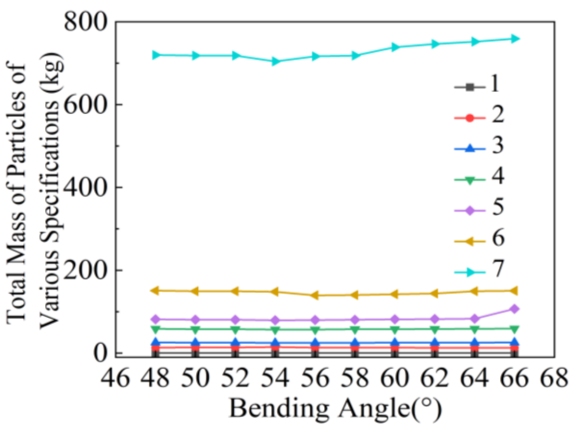

Figure 6: Influence of bending angle on mass of particles with different specifications.

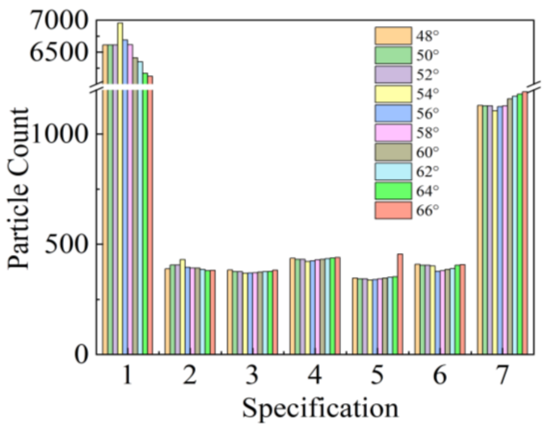

Figure 7: Influence of bending angle on number of particles with different specifications.

4.2 Analysis of blade tip thickness data for different blades at the bending angle of 54°

Fig. 8 shows that when the blade tip thickness was 2.0–4.0 mm, the total number of particles mostly showed a trend of first increasing and then decreasing with the increase in the tip thickness of the rotary blade. In the 1st, 4th, and 6th experiment, the maximum total particle number was reached at the blade tip thickness of 3.0 mm. In the 5th and 8th experiment, the maximum total particle number was achieved at the blade tip thickness of 3.5 mm. In the 3rd experiment, the total particle number was the highest at the blade tip thickness of 2.5 mm. In the 2nd and 7th experiment, the total particle number was the highest at the blade tip thickness of 2.0 mm. The data from 8 experiments were averaged, and the total particle number peaked at the blade tip thickness of 3.0 mm. The total particle number under the declining blade tip thickness was approximately equal to that under the increasing blade tip thickness, that is, when the blade tip thickness of 3.0 mm was taken as the benchmark, the increasing blade tip thickness influenced the total particle number in a similar manner as the declining blade tip thickness did. Comparative analysis of Figs. 6 and 8 reveals that within the ranges of the bending angle (48°–66°) and the blade tip thickness (2.0–4.0 mm), the bending angle had a greater effect on the total number of particles than the blade tip thickness.

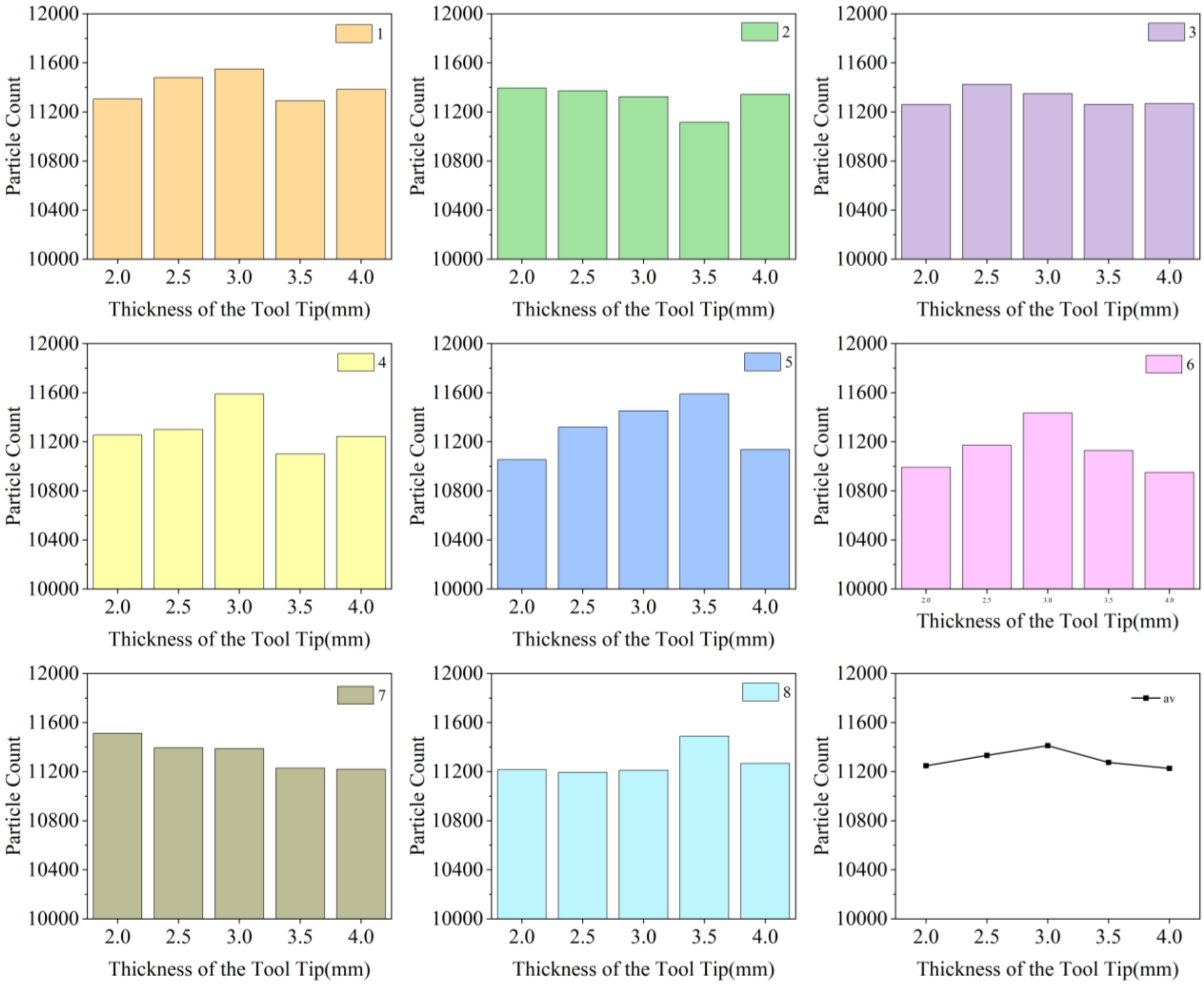

Figure 8: Particle number at different blade tip thicknesses and blade bending angle of 54°.

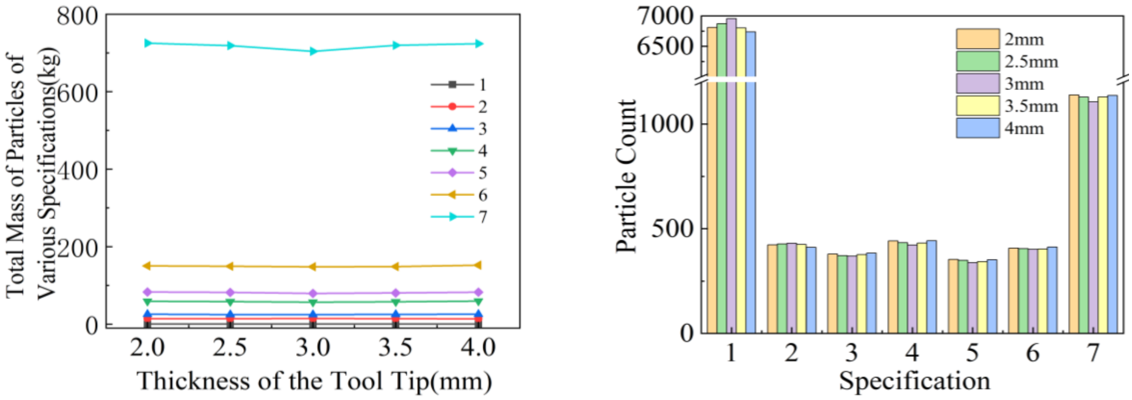

a) Mass of different specifications b) Number of different specifications

Figure 9: The mass and number of particles of different specifications under different blade tip thicknesses and a 54° blade curvature angle.

As shown in Fig. 9 a, under a constant blade tip thickness (2.0–4.0 mm), the particle mass of Specifications 1–7 increased progressively. With increasing blade tip thickness, the mass of Specifications 1 and 2 first rose and then fell, peaking at 3.0 mm, while the mass of Specifications 3–7 first decreased and then increased, reaching a minimum at 3.0 mm. Fig. 9 b indicates that across the same thickness range, Specification 1 had the highest particle count, followed by Specification 7. Integrating both figures reveals that at 3.0 mm blade tip thickness, Specification 1 reached its maximum particle number, while Specifications 3–7 accounted for the lowest proportion of total mass-indicating minimal presence of high-mass particles. Since Specifications 1 and 2 represent the smallest unit particle mass, their high quantity and low mass reflect effective fragmentation. Thus, the combination of a 54° bending angle and 3.0 mm blade tip thickness is identified as optimal, producing the highest total particle number and the lowest proportion of high-mass particles.

4.3 Comparative analysis of breakage effect under optimal conditions and standard conditions

The number of particles with different specifications and the particle mass at the bending angle of 54° and blade tip thickness of 3.0 mm and under standard conditions (bending angle: 60° and blade tip thickness: 3.0 mm) are listed in Tables III and IV. Table V reveals that at the blade tip thickness of 3.0 mm, at a bending angle of 54° was greater than that at the bending angle of 60° in eight experiments; the average particle number was increased by 5.14 %.

Tables IV and V present that at the blade tip thickness of 3.0 mm, the total particle mass of Specifications 1–7 gradually increased as the individual particle mass increases; the total particle mass and particle number of Specifications 1, 2, and 6 at the bending angle of 54° were greater than those at the bending angle of 60°, and those of Specifications 3, 4, 5, and 7 presented the opposite trend; at the bending angle of 54°, Specifications 1 and 2 with small individual particle masses showed greater particle numbers, the breakage effect of small particles was good, the total mass of large particles of Specifications 3–7 accounted for a smaller proportion of the total mass ratio among the seven specifications, and the rotary tillage effect was evidently improved after optimization. The included angle between the blade and soil (cutting angle) affected the cutting resistance and soil breakage effect, and a reasonable cutting angle weakened the cutting resistance, improved the cutting efficiency, and further elevated the soil breakage rate.

Table III: Influence of bending angle on particle number.

Bending angle	**Particle number in each experiment**								**Average particle number**
	1	**2**	**3**	**4**	**5**	**6**	**7**	**8**	
54°	11549	11324	11349	11588	11453	11434	11388	11211	11412
60°	10867	10701	10841	11105	11056	10822	10659	10786	10854

Table IV: Influence of bending angle on particle mass of different specifications.

Bending angle	**Total mass of particles with all specifications** (kg)						
	1	**2**	**3**	**4**	**5**	**6**	**7**
54°	0.3881	14.4658	24.7491	56.5842	79.2978	148.1929	704.1891
60°	0.3578	13.1568	25.0845	57.9251	81.4093	142.2947	738.5708

Table V: Influence of bending angle on particle number of different specifications.

Bending angle	**Number of particles with different specifications**						
	1	**2**	**3**	**4**	**5**	**6**	**7**
54°	6956	431	369	422	338	402	1106
60°	6413	392	374	432	347	386	1160

To sum up, regarding parameter optimization, the bending angle of 54° and the blade tip thickness of 3.0 mm were determined as the optimal parameter combination. Under these conditions, the total number of broken soil particles reached its peak. The breakage of small particles (Specifications 1 and 2) was the most pronounced, whereas the proportion of the high-mass particles (Specifications 3–7) decreased to its minimum level. Compared with common standard conditions (bending angle: 60° and blade tip thickness: 3.0 mm) in engineering, this optimization scheme increased the total particle number by an average of 5.14 % and effectively improved the uniformity and fragmentation degree of soil particles.

From the perspective of parameter interaction, the bending angle was the dominant factor, exerting a significantly greater influence on total particle number than blade tip thickness. Both parameters exhibited a highly consistent synergistic effect on particle distribution: under optimal conditions, the mass and number of small particles (Specifications 1–2) peaked, while the mass of large particles (Specifications 3–7) reached a minimum. This indicates that the optimal parameter combination simultaneously promotes fine particle generation and suppresses large clod formation. The bending angle primarily regulates breakage by influencing the cutting angle and soil throwing. A 54° bending angle likely provides an ideal cutting angle, reducing resistance and enhancing secondary breakage by optimizing soil tearing and throwing. Meanwhile, blade tip thickness mainly affects stress concentration and extrusion. A thickness of 3.0 mm achieves the best balance between sharpness and structural strength, effectively converting cutting force into tensile stress for soil breakage while avoiding over-compaction.

In this study, simulations of loess soil were conducted in EDEM under multiple parameter combinations, and the experimental data were analysed. The best soil breakage effect and optimal tillage were achieved at the bending angle of 54° and blade tip thickness of 3.0 mm. This configuration enabled the tool to cut into the soil smoothly with low resistance and fully break the furrow slice through an effective wedging action, followed by secondary breakage during the throwing. Consequently, energy was applied to create new particle surfaces to the greatest extent, which remarkably improved the energy efficiency of soil breakage.

5. CONCLUSIONS

To improve the soil quality of cultivated land effectively and to reveal the action mechanism between the structural parameters of the rotary blade and the soil particle breakage effect, the influence laws of the rotary blade's bending angle and blade tip thickness on soil particle breakage were explored first. Then, the rotary tillage was simulated under different parameter combinations using the discrete element method. Afterward, the soil breakage effect was comparatively verified under the optimized parameters and the traditional standard parameters. Finally, the following conclusions were drawn.

(1) The bending angle of the rotary blade is the dominant factor affecting the total soil particle number. The total soil particle number first increases and then declines with the increase in the bending angle and exhibits the same trend with the increase in the blade tip thickness.

(2) Under the set simulation conditions, the optimal parameter combination of the rotary blades was a bending angle of 54° and a blade tip thickness of 3.0 mm. Under these conditions, the fine soil particle number grows markedly, and the mass ratio of large particles is the minimal.

(3) Compared with the standard parameters (bending angle: 60° and blade tip thickness: 3.0 mm), the average particle number under the optimal parameter combination increases by 5.14 %, and the soil breakage effect is considerably better. By promoting the full breakage of soil particles, the optimal parameter combination elevates the ratio of fine particles, improves the soil structure, and further conforms to the requirements of agricultural intensive cultivation for soil fragmentation.

In this study, simulation combined with the theoretical analysis was adopted, and a discrete element model of rotary blade–soil interaction was established. This model can accurately simulate the motion and breakage of soil particles and provide a reliable theoretical basis and data analysis tools for the parameter design and optimization of rotary blades and is of great guiding value for improving the quality of cultivated land in North China. In this study, only the soil breakage data in the rotary tillage of soil were examined, and an analysis was made combining the existing laws. However, the coupling mechanism of the rotary blade parameters in soil breakage was not deeply explored. In the follow-up study, the stress borne by soil in the rotary tillage and the soil breakage mechanism will be further investigated.

ACKNOWLEDGEMENT

This study was funded by the Bijie City Science and Technology Project of China (Grant No. BKLH [2025]-6), and the Scientific and Technological Innovation Team of Higher Education Institutions under the Education Department of Guizhou of China (Grant No. QJJ [2023]093).

REFERENCES

[1] Molotoks, A.; Smith, P.; Dawson, T. P. (2021). Impacts of land use, population, and climate change on global food security, *Food and Energy Security*, Vol. 10, No. 1, Paper e261, 20 pages, doi:10.1002/fes3.261

[2] Zhu, Y.-Y.; Wang, Z.-W.; Zhu, X.-H. (2023). New reflections on food security and land use strategies based on the evolution of Chinese dietary patterns, *Land Use Policy*, Vol. 126, Paper 106520, 11 pages, doi:10.1016/j.landusepol.2022.106520

[3] Montgomery, D. R. (2024). Soil security and global food security, *Frontiers of Agricultural Science and Engineering*, Vol. 11, No. 2, 297-302, doi:10.15302/J-FASE-2023530

[4] Kulaya, P. W.; Yadav, S. N. (2021). Study on tillage quality and energy requirement of 'L' and 'C' profile rotary tiller blades for clayey soil of Sikkim under soil bin condition, *Journal of Agricultural Engineering (India)*, Vol. 58, No. 4, 309-322, doi:10.52151/jae2021581.1754

[5] Zykin, E.; Lazutkina, S. (2022). Determination of the operating mode of the tillage unit with rotary blades, *AIP Conference Proceedings*, Vol. 2503, No. 1, Paper 030040, doi:10.1063/5.0099994

[6] Li, Q. (2023). Green supply chain optimization with fuzzy MCDM for economic growth, *International Journal of Simulation Modelling*, Vol. 22, No. 4, 690-700, doi:10.2507/IJSIMM22-4-CO16

[7] Wang, X.-Z.; Geng, L.-X.; Zhou, H.-M.; Huang, Y.-X.; Ji, J.-T. (2023). Effects of subsoiling with different wing mounting heights on soil water infiltration using HYDRUS-2D simulations, *Agronomy*, Vol. 13, No. 11, Paper 2742, 13 pages, doi:10.3390/agronomy13112742

[8] Gupta, G. S. (2019). Land degradation and challenges of food security, *Review of European Studies*, Vol. 11, No. 1, 63-72, doi:10.5539/res.v11n1p63

[9] Hoseinian, S. H.; Hemmat, A.; Esehaghbeygi, A.; Shahgoli, G.; Baghbanan, A. (2022). Development of a dual sideway-share subsurface tillage implement: Part 2. Effect of tool geometry on tillage forces and soil disturbance characteristics, *Soil and Tillage Research*, Vol. 215, Paper 105200, 10 pages, doi:10.1016/j.still.2021.105200

[10] Patidar, P.; Soni, P.; Jain, A.; Mahore, V. (2024). Modelling soil-rotor blade interaction of vertical axis rotary tiller using discrete element method (DEM), *Journal of Terramechanics*, Vol. 112, 59-68, doi:10.1016/j.jterra.2024.01.001

[11] Jin, H.; Huang, S.; Shi, D.; Li, J.; Li, J., Li, Y.; Zhu, H. (2023). Effects of different tillage practices on soil stability and erodibility for red soil sloping farmland in southern China, *Agronomy*, Vol. 13, No. 5, Paper 1310, 22 pages, doi:10.3390/agronomy13051310

[12] Adekiya, A. O.; Adedokun, O. D., Adebiyi, O. T. (2024). Soil characteristics, growth, yield, mineral composition and proximate content of soybeans under various tillage techniques, *International Journal of Agronomy*, Vol. 2024, Paper 006392, 13 pages, doi:10.1155/2024/2006392

[13] Janusauskaite, D.; Kadziene, G. (2022). Influence of different intensities of tillage on physiological characteristics and productivity of crop-rotation plants, *Plants*, Vol. 11, No. 22, Paper 3107, 15 pages, doi:10.3390/plants11223107
[14] Al-Shammary, A. A. G.; Al-Shihmani, L. S. S.; Fernández-Gálvez, J.; Caballero-Calvo, A. (2024). Optimizing sustainable agriculture: a comprehensive review of agronomic practices and their impacts on soil attributes, *Journal of Environmental Management*, Vol. 364, Paper 121487, 28 pages, doi:10.1016/j.jenvman.2024.121487
[15] San, Y. L.; Li, Y. M.; Xiao, S. H.; Zhang, C. Y.; Liu, Y. B. (2024). Parameter optimization and analysis of plastic separator based on EDEM-Fluent, *International Journal of Simulation Modelling*, Vol. 23, No. 4, 622-633, doi:10.2507/IJSIMM23-4-701
[16] Shaikh, S. A.; Li, Y.; Ma, Z.; Chandio, F. A.; Tunio, M. H.; Liang, Z.; Solangi, K. A. (2021). Discrete element method (DEM) simulation of single grouser shoe-soil interaction at varied moisture contents, *Computers and Electronics in Agriculture*, Vol. 191, Paper 106538, 8 pages, doi:10.1016/j.compag.2021.106538
[17] Nalawade, R. D.; Singh, K. P.; Roul, A. K; Agrawal, K. N.; Sonawane, S.; Mahore, A.; Patel, A.; Kumar, M.; Shelake, P.; Salem, A.; Elbeltagi, A. (2024). Study on the effect of geometrical and operational parameters on performance dynamics of modified rotary blades using DEM, *Scientific Reports*, Vol. 14, Paper 19239, 21 pages, doi:10.1038/s41598-024-69803-8
[18] Xiao, W.; Niu, P.; Wang, P.; Xie, Y.; Xia, F. (2024). Simulation analysis and optimization of soil cutting of rotary blade by Ansys/Ls-Dyna, *INMATEH – Agricultural Engineering*, Vol. 72, No. 1, 22-32, doi:10.35633/inmateh-72-02
[19] Zhao, H.; Li, H.; Ma, S.; He, J.; Wang, Q.; Lu, C.; Zheng, Z.; Zhang, C. (2020). The effect of various edge-curve types of plain-straight blades for strip tillage seeding on torque and soil disturbance using DEM, *Soil and Tillage Research*, Vol. 202, Paper 104674, 11 pages, doi:10.1016/j.still.2020.104674
[20] Sun, J.; Wang, Y.; Ma, Y.; Tong, J.; Zhang, Z. (2018). DEM simulation of bionic subsoilers (tillage depth >40 cm) with drag reduction and lower soil disturbance characteristics, *Advances in Engineering Software*, Vol. 119, 30-37, doi:10.1016/j.advengsoft.2018.02.001
[21] Wang, L.; Guo, H.; Wang, L.; Cheng, D. (2022). Suitable tillage depth promotes maize yields by changing soil physical and chemical properties in a 3-year experiment in the North China Plain, *Sustainability*, Vol. 14, No. 22, Paper 15134, 16 pages, doi:10.3390/su142215134
[22] Islam, M. U.; Jiang, F.; Halder, M.; Barman, A.; Liu, S.; Peng, X. (2024). Quantitative assessment of different straw management practices on soil organic carbon and crop yield in the Chinese upland soils: a data-driven approach based on simulation and prediction model, *European Journal of Agronomy*, Vol. 154, Paper 127092, 13 pages, doi:10.1016/j.eja.2024.127092
[23] Zheng, F.; Liu, X.; Ding, W.; Song, X.; Li, S.; Wu, X. (2023). Positive effects of crop rotation on soil aggregation and associated organic carbon are mainly controlled by climate and initial soil carbon content: a meta-analysis, *Agriculture Ecosystems & Environment*, Vol. 355, Paper 108600, 13 pages, doi:10.1016/j.agee.2023.108600
[24] Yazdani, E.; Hashemabadi, S. H.; Taghizadeh, A. (2021). Investigation of particulate bed dynamics inside a rotating drum using discrete element method, *Particulate Science and Technology*, Vol. 39, No. 8, 917-927, doi:10.1080/02726351.2020.1870595
[25] Zhao, C.; Wu, X. (2019). Analysis of soil fertilizer mixing process based on EDEM discrete element method, *Journal of Chinese Agricultural Mechanization*, Vol. 40, No. 7, 178-182, doi:10.13733/j.jcam.issn.2095-5553.2019.07.31
[26] Wang, B.; Chen, M.; Wei, J.; Liang, G.; Liang, K. (2022). Bionic optimization design of rotary tiller based on fuzzy algorithm, *Mobile Information Systems*, Vol. 2022, Paper 1203973, 11 pages, doi:10.1155/2022/1203973
[27] China Machinery Industry Federation. Rotary cultivator GB/T 5668-2017, from *http://c.gb688.cn/bzgk/gb/showGb?type=online&hcno=C4A5376BA5C4F93CF353E9BD73DB7E99*, accessed on 29-09-2017